

---

This is an electronic reprint of the original article.

This reprint may differ from the original in pagination and typographic detail.

Jonkergouw, Christopher; Savola, Pihla; Osmekhina, Ekaterina; van Strien, Joeri; Batys, Piotr; Linder, Markus B.

**Exploration of Chemical Diversity in Intercellular Quorum Sensing Signalling Systems in Prokaryotes**

*Published in:*

Angewandte Chemie - International Edition

*DOI:*

[10.1002/anie.202314469](https://doi.org/10.1002/anie.202314469)

Published: 08/01/2024

*Document Version*

Publisher's PDF, also known as Version of record

*Published under the following license:*

CC BY

*Please cite the original version:*

Jonkergouw, C., Savola, P., Osmekhina, E., van Strien, J., Batys, P., & Linder, M. B. (2024). Exploration of Chemical Diversity in Intercellular Quorum Sensing Signalling Systems in Prokaryotes. *Angewandte Chemie - International Edition*, 63(2), Article e202314469. <https://doi.org/10.1002/anie.202314469>

---

This material is protected by copyright and other intellectual property rights, and duplication or sale of all or part of any of the repository collections is not permitted, except that material may be duplicated by you for your research use or educational purposes in electronic or print form. You must obtain permission for any other use. Electronic or print copies may not be offered, whether for sale or otherwise to anyone who is not an authorised user.

**Bacterial Signalling**


# Exploration of Chemical Diversity in Intercellular Quorum Sensing Signalling Systems in Prokaryotes

Christopher Jonkergouw, Pihla Savola, Ekaterina Osmekhina, Joeri van Strien, Piotr Batys, and Markus B. Linder\*

**Abstract:** Quorum sensing (QS) serves as a vital means of intercellular signalling in a variety of prokaryotes, which enables single cells to act in multicellular configurations. The potential to control community-wide responses has also sparked numerous recent biotechnological innovations. However, our capacity to utilize intercellular communication is hindered due to a scarcity of complementary signalling systems and a restricted comprehension of interconnections between these systems caused by variations in their dynamic range. In this study, we utilize uniform manifold approximation and projection and extended-connectivity fingerprints to explore the available chemical space of QS signalling molecules. We investigate and experimentally characterize a set of closely related QS signalling ligands, consisting of *N*-acyl homoserine lactones and the aryl homoserine lactone *p*-coumaroyl, as well as a set of more widely diverging QS ligands, consisting of photopyrones, dialkylresorcinols, 3,5-dimethylpyrazin-2-ol and autoinducer-2, and define their performance. We report on a set of six signal- and promoter-orthogonal intercellular QS signalling systems, significantly expanding the toolkit for engineering community-wide behaviour. Furthermore, we demonstrate that ligand diversity can serve as a statistically significant tool to predict much more complicated ligand-receptor interactions. This approach highlights the potential of dimensionality reduction to explore chemical diversity in microbial dynamics.

## Introduction

Cellular cooperation forms one of the defining features of higher organisms. The differentiation into various cell types allows cells to divide tasks and specialize.<sup>[1]</sup> Prokaryotes have also developed methods to organize more complex architectures. Bacteria utilize small molecules in quorum sensing (QS) as a form of intercellular signalling, which enables them to synchronize and organize behaviour on a population-wide or even community-wide level<sup>[2]</sup> to facilitate bacterial biofilm architectures,<sup>[3]</sup> promote plant colonization,<sup>[4]</sup> or commence the production of a range of virulence factors.<sup>[5]</sup> Consequently, these intercellular signalling systems have attracted widespread interest in biotechnology, where the potential to control community-wide responses has sparked innovations in microbiome therapeutics,<sup>[6]</sup> microbial factories,<sup>[7]</sup> and cellular computing.<sup>[8]</sup> Continually, novel ligands, receptors and whole signalling systems are being identified and characterized,<sup>[9]</sup> proposedly advancing our understanding of natural multicellular communities and expanding the toolkit for biotechnological innovation. However, a key challenge that remains, given the wide diversity in identified ligands, receptors, and signalling classes, is in advancing the understanding of non-cognate binding in these signalling systems, and in the identification of differences in their dynamic range.

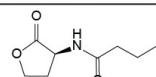
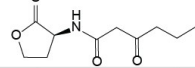
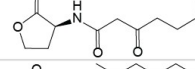
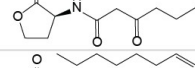
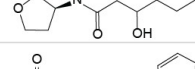
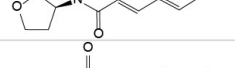
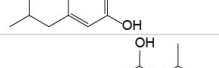
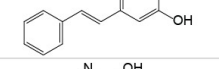
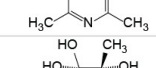
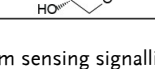
QS signalling systems and ligands, despite having large individual differences, share common features.<sup>[10]</sup> QS systems consist of an intracellular synthase gene of either the QS signalling molecule or a precursor molecule. The ligand is bound by a receptor protein. The binding results in conformational changes, enabling the receptor-ligand complex to bind a promoter, which results in gene regulatory changes.<sup>[11]</sup> Here, we move beyond the commonly utilized HSL QS signalling systems and explore how chemical diversity in ligands can serve as a guiding principle to understand and circumvent non-cognate binding interactions. We explore the chemical diversity in a comprehensive set of known QS ligands and, based on the hypothesis that diversity in ligand chemical structures minimizes non-cognate interactions, experimentally assess a set of structurally similar as well as a diverging set of QS signalling systems (Figure 1). Using this approach, we significantly expand upon the known and available synthetic orthogonal QS signalling systems and provide a clear strategy towards future expansion efforts of additional synthetic orthogonal signalling systems.

[\*] C. Jonkergouw, P. Savola, E. Osmekhina, M. B. Linder  
Aalto University, School of Chemical Engineering, Department of Bioproducts and Biosystems  
Kemistintie 1, 02150 Espoo (Finland)  
E-mail: markus.linder@aalto.fi

J. van Strien  
Medical BioSciences Department, Radboud University Medical Center  
Geert Grooteplein 28, 6525 GA Nijmegen (The Netherlands)

P. Batys  
Jerzy Haber Institute of Catalysis and Surface Chemistry, Polish Academy of Sciences  
Niezapominajek 8, 30239 Krakow (Poland)

© 2023 The Authors. Angewandte Chemie International Edition published by Wiley-VCH GmbH. This is an open access article under the terms of the Creative Commons Attribution License, which permits use, distribution and reproduction in any medium, provided the original work is properly cited.

Molecular Structure	Short name	Signalling system	Origin
	C4 HSL	Rhl	<i>Pseudomonas aeruginosa</i>
	3-oxo-C6 HSL	Lux	<i>Vibrio fischeri</i>
	3-oxo-C8 HSL	Tra	<i>Agrobacterium tumefaciens</i>
	3-oxo-C12 HSL	Las	<i>Pseudomonas aeruginosa</i>
	3-OH-C14:1 HSL	Cin	<i>Rhizobium leguminosarum</i>
	pC HSL	Rpa	<i>Rhodopseudomonas palustris</i>
	PPYA	Plu	<i>Photobacterium luminescens</i>
	IPS	Pau	<i>Photobacterium asymbiotica</i>
	DPO	Vqm	<i>Vibrio cholerae</i>
	AI-2 (R-THMF)	Lsr	Multiple species

**Figure 1.** Different quorum sensing signalling systems explored in this study. QS signalling systems were chosen based on the variation of their chemical structures. The signalling molecules, inducible promoter, synthase genes and corresponding receptors are C4 HSL/*Prhl*/*RhlI*/*RhlR* from *Pseudomonas aeruginosa*, 3-oxo-C6 HSL/*Plux*/*LuxI*/*LuxR* from *Vibrio fischeri*, 3-oxo-C8 HSL/*Ptra*/*TraI*/*TraR* from *Agrobacterium tumefaciens*, 3-oxo-C12 HSL/*Plas*/*LasI*/*LasR* from *Pseudomonas aeruginosa*, 3-OH-C14:1 HSL/*Pcin*/*CinI*/*CinR* from *Rhizobium leguminosarum*, pC HSL/*Prpa*/*RpaI*/*RpaR* from *Rhodopseudomonas palustris*, PPYA/*PpcfA-L*/*PpyS*/*PluR* from *Photobacterium luminescens*, IPS/*PpcfA-A*/*DarABC*/*PauR* from *Photobacterium asymbiotica*, DPO/*PvqmR*/*Tdh*/*VqmA* from *Vibrio cholerae* and AI-2/*Plsr*/*LuxS*/*LsrABC*, *LsrK* and *LsrR* from a wider variety of bacterial species. The six classes of QS signalling molecules presented here are *N*-acyl homoserine lactones (acyl-HSLs; R=O, OH/H, or H/H), aryl homoserine lactone *p*-coumaroyl-HSL, photopyrones, dialkylresorcinols, 3,5-dimethylpyrazin-2-ol (DPO) and furanosylborate diester autoinducer-2 (AI-2).

## Results and Discussion

To explore the structural diversity present in signalling molecules across various QS systems, we investigated a comprehensive set of 166 known signalling molecules used by prokaryotes, as previously classified in seven structurally distinct classes; homoserine lactones (HSLs), autoinducer-2 (AI-2 s), Diffusible signalling factors (DSFs), 4-hydroxy-2-alkylquinolines (HAQs), *n*-fatty acid methyl esters (NAMEs) diketopiperazines (DKPs) and a category of QS signalling systems that cannot be placed in the other classes called “Others” (Supplementary Table 1).<sup>[12]</sup> To systematically determine the structural similarity between this collection of signalling molecules and the different classes, extended-connectivity fingerprints (ECFP) fingerprints were generated for each molecule. The structural similarity between all signalling molecule pairs was estimated by computing the Tanimoto similarity between the respective fingerprints (Figure 2a).<sup>[13]</sup> To provide an overview of the structural diversity present in this collection of signalling molecules, the pairwise Tanimoto similarities were used as

input for uniform manifold approximation and projection (UMAP) dimensional reduction (Figure 2b).<sup>[14]</sup> This UMAP projection of all QS ligands shows large variations, i.e., structural diversity, between most QS classes. DSFs, HAQs and NAMEs are all distinctly separated from other classes. Furthermore, DKPs, DSFs and NAMEs exhibit a high degree of structural similarity within their respective classes. HAQ ligands, while structurally distinct from other classes, exhibit a larger variation in individual ligands. HSLs display a high degree of structural similarity, where a zoom-in reveals three clusters of HSL ligands (Figure 2c). The HSLs with a carbonyl group, 3-oxo-C6, 3-oxo-C8 and 3-oxo-C12 are all closely overlapping, as well as the HSLs with a hydroxyl group 3-OH-C14:1 (Figure 2d). Surprisingly, the AI-2 ligand *R*-THMF shows a high degree of structural similarity with HSL ligands, whereas its precursor, DPD, is structurally divergent (Figure 2c,e). Signalling molecules characterized as “Others”, a group of ligands that structurally fall outside other classifications, show larger variations compared to ligands in the same class, while also overlapping with ligands from the DKP and AI-2 classes (Fig-

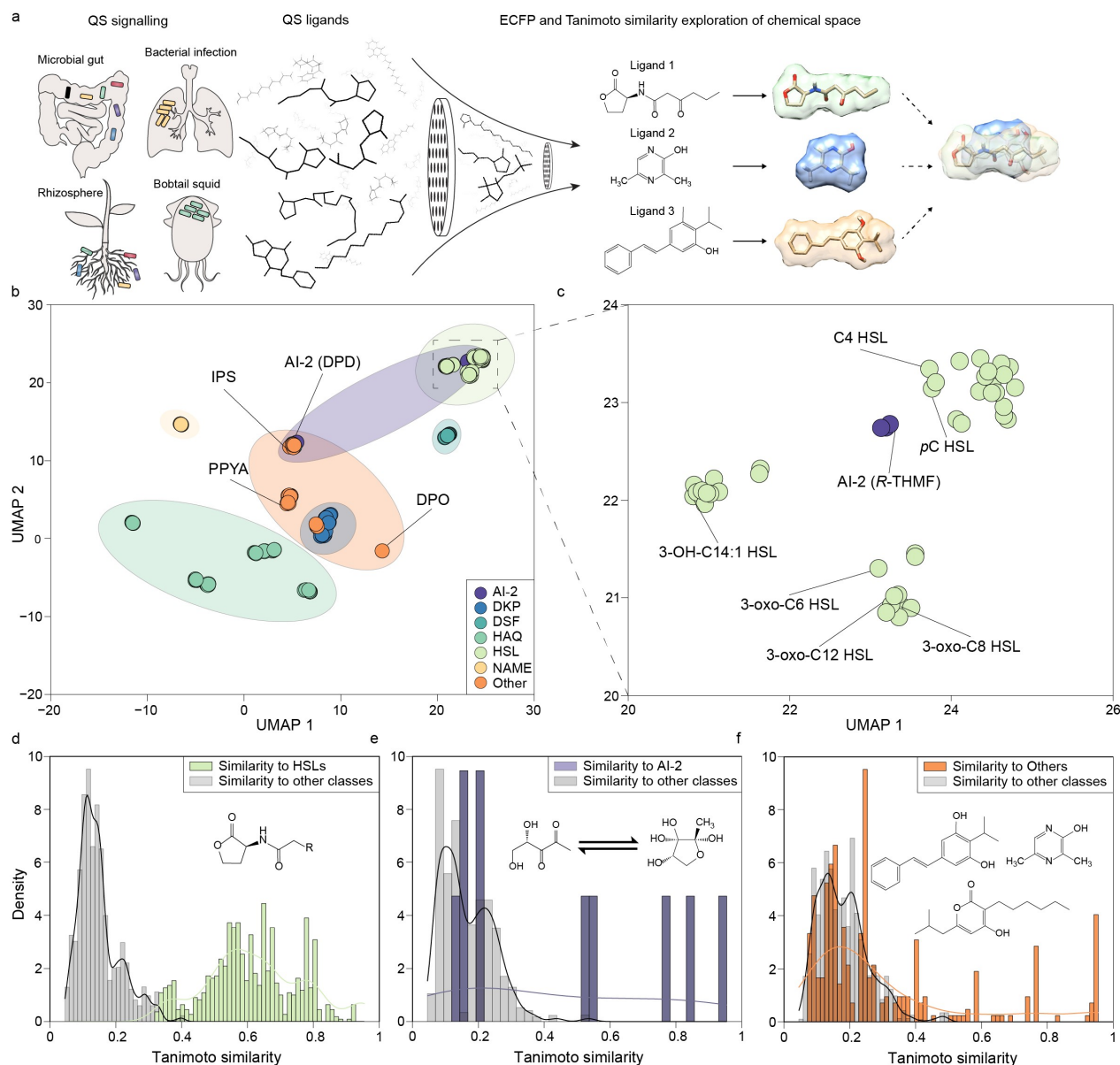


**Figure 2.** Exploration of chemical diversity in quorum sensing ligands. a) Extended-Connectivity Fingerprint and Tanimoto similarity exploration of chemical space using a diverse set of QS signalling molecules, comprising 166 unique ligands. Most signalling molecules were obtained from the Sigmol repertoire of quorum sensing signalling molecules in prokaryotes. b) Visual exploration of QS signalling molecule diversity, with ligands represented as ECFPs. Tanimoto similarities are used for the UMAP dimensionality reduction. QS systems experimentally explored in this study are labelled. Because the reactions that lead to the biologically active form of AI-2, (2R,4S)-2-methyl-2,3,3,4-tetrahydroxytetrahydrofuran (*R*-THMF), are reversible, the precursor molecule, 4,5-dihydroxy-2,3-pentanedione (DPD), is also labelled. c) Zoom-in of QS ligand Tanimoto UMAP, as seen in (b), showing the large structural similarities between the HSL QS ligands. Besides the HSLs, three of the AI-2 ligands show large overlaps with the HSL ligands. QS systems experimentally explored in this study are labelled. d) Similarity comparison between HSLs and other classes shows a high degree of overlap among individual “HSL” ligands, and a low similarity to QS ligands in other classes. Highlighted in the graph is the conserved part of HSLs used in this study as marked in (b,c), a lactone unit, connected to the carbonyl acyl chain of variable length, (R). Of the ligands used in this study, the acyl chain ranges from 4–14 carbons. e) Similarity comparison between “AI-2” ligands and other classes shows large variations in the overlap between individual AI-2 ligands, with some AI-2 ligands highly similar and some ligands distinctly different. Highlighted in the graph, as marked in (b,c), are the precursor and the active form of AI-2, *R*-THMF. f) Similarity comparison between “Others” ligands and other classes shows large variations in the overlap between individual ligands in this class. Since the category contains more diverse and difficult to categorize structures, the “Others” ligands show both low and large similarity within its own class, and an increased overall similarity compared to other classes. Highlighted in the graph are the ligands in the category “Others” used in this study, as marked in (b), PPYA, IPS and DPO.

ure 2f). The larger variation within its class is in line with expectations, since the class contains all QS ligands that do not fit other classes.

Next, we selected a cluster of signalling molecules of which the ligands show high structural similarity. The most studied, characterized and utilized QS systems are *N*-acyl



HSLs, which consist of a conserved homoserine lactone that is connected to an acyl chain of variable length, ranging from 4 to 18 carbons.<sup>[15]</sup> The third carbon can either be fully reduced or contain a carbonyl/hydroxyl group. We selected five *N*-acyl HSLs to represent the ligand diversity, both in chain length (C4–C14) and third carbon functionalization and included the C4/RhlR signalling system from *Pseudomonas aeruginosa*,<sup>[16]</sup> the 3-oxo–C6/LuxR signalling system from *Vibrio fischeri*,<sup>[9a,17]</sup> the 3-oxo–C8/TraR signalling system from *Agrobacterium tumefaciens*,<sup>[18]</sup> the 3-oxo–C12/LasR signalling system also from *Pseudomonas aeruginosa* and the 3OH–C14:1/CinR signalling system from *Rhizobium leguminosarum* (Figure 3a).<sup>[19]</sup> In addition to these, we included a QS system from *Rhodopseudomonas palustris*, which utilizes an aryl HSL, *p*-Coumaroyl (*pC*) HSL, *pC*/RpaR. *p*-C also shares the homoserine lactone unit of *N*-acyl HSLs, but contains a phenol group at the acyl chain terminus.<sup>[4b,20]</sup> Similar to *N*-acyl HSLs, it requires S-adenosyl-L-methionine as a precursor. However, it also requires the plant-derived lignin precursor *p*-coumaric acid (Figure 3a, right precursor). As a result, this type of QS communication can only occur during plant colonization, where/when the precursor is present in the environment.<sup>[21]</sup> Next, we constructed a set of synthetic *E. coli*-based sensory strains for each of the HSL signalling systems (Figure 3b, Supplementary Table 2).

As previously reported, the LuxR receptor is activated by all other HSLs, including the Aryl HSL *pC* (Figure 3c).<sup>[22]</sup> Surprisingly, the strongest and most sensitive activation was observed not with its cognate ligand, 3-oxo–C6, but with the structurally very similar 3-oxo–C8 HSL. Also, no steric hindrance occurs with 3-oxo–C12, a ligand that contains two times longer aliphatic chain compared to its cognate ligand, 3-oxo–C6. The Aryl *pC* HSL receptor RpaR is strongly activated by its cognate ligand, with mild to moderate activation in the presence of other HSL ligands, although only in the highest concentration  $1\text{E}^{-4}\text{ M}$  (Figure 3d). We challenged the HSL signalling systems with a set of non-HSL ligands (Figure 3e). Interestingly, none of the ligands could activate any of the HSL signalling systems, suggesting that exploring structural diversity is a promising approach to minimize non-cognate recognition between ligand-receptor pairs. Although *E. coli* does not utilize HSL QS signalling systems, it does express a LuxR orphan receptor (without cognate ligand) called SdiA. This receptor is known to bind a range of non-cognate ligands and can result in elevated background activation of HSL based QS systems, which we also observed (Figure 3e, zoom-in).<sup>[21b,23]</sup> For this reason, a  $\Delta\text{sdiA}$  knockout strain, CY008, was used for all HSL signalling characterizations. A comparison of all HSL QS systems shows considerable differences in overall strength of the activation and sensitivity of the response, with the activation of 3-oxo–C6/LuxR and *pC*/RpaR being stronger and more sensitive, and the activation of C4/RpaR and 3-oxo–C8/TraR being weaker and less sensitive (Figure 3f).

Next, we used all-atom Molecular Dynamics (MD) simulations to further investigate the binding of non-cognate ligands at high ligand concentrations. The simulations show how the non-cognate ligand 3-oxo–C12 can easily enter to

the LuxR receptor pocket and bind specifically to it via the HSL group (Figure 3, Supplementary video 1). The binding of 3-oxo–C6 to the RpaR receptor at high ligand concentration has also been confirmed via MD simulations, although a longer simulation time was needed to observe it (Supplementary video 2). Figure 3h shows that the ligand binds via the HSL group to the tryptophan amino acid in the RpaR receptor pocket. As only one oxygen atom in the HSL group was found to be involved in binding, one can expect the binding to be relatively weak, as was observed experimentally (Figure 3d).

We then turned to the QS signalling systems that are placed far away from the *N*-acyl and Aryl QS ligands in the Tanimoto similarity map, categorized as “Others”. This group of ligands is not only divergent from HSLs, but there is also large structural diversity within the group itself. From this group, we first focused on two more recently described novel QS signalling systems in *Photobacterium* species, where they both play an important part in cell clumping and pathogenicity: the IPS/PauR signalling system from *Photobacterium asymbiotica*<sup>[9b]</sup> and the PPYA/PluR signalling system from *Photobacterium luminescens*.<sup>[24]</sup> The LuxR-type receptor PauR senses dialkylresorcinols (DARs), as well as its corresponding cyclohexanedione (CHD) precursors, which bind to the promoter *PpcfA–A*, activating the expression of the *pcfABCDEF* operon (Figure 4a). The DarABC operon produces a specific subset of DARs (6) and their chemical precursors CHDs (Figure S1a).<sup>[25]</sup> The LuxR-type receptor PluR senses a group of  $\alpha$ -pyrones named photopyrones (PPYs), which bind to the promoter *PpcfA–L*, also activating the expression of the *pcfABCDEF* operon. PPYs consist of a central  $\alpha$ -pyrone ring that is modified with two iso-branched hydrophobic side chains of variable length. The synthase *PpyS* produces a specific subset of PPYs (8) (Figure S1a). We used a single ligand for induction of each system; IPS for receptor PauR and PPYA for receptor PluR (supplementary Figure 1, highlighted in bold). We started with the introduction of both receptor proteins and promoters into *E. coli* strain CY008. However, constitutive expression of both receptor proteins resulted in a lack of colonies after transformation. Extensive screening from multiple ligation and transformation attempts generated a limited number of colonies that all contained non-synonymous mutations, resulting in amino acid substitutions. In the case of PauR, four sequenced colonies (from different ligations and transformations) all contained a point mutation in S129 a serine involved in AHL binding, within the autoinducer binding domain (Figure S2). Four clones of PluR contained non-synonymous mutations, all resulting also in amino acid substitutions. We hypothesized that constitutive expression severely affects viability in *E. coli*, so to overcome this, we controlled the expression of the receptor proteins with *L*-rhamnose (Figure 4b). This resulted in functional (and sequencing verified) constructs that we were able to experimentally assess. We first validated the range of activation of PauR with varying concentrations of *L*-rhamnose (Figure 4c, top/right panel). The highest concentration ( $1\text{ }\mu\text{M}$ ) resulted in a negative effect on the bacterial viability ( $\text{OD}_{600}$ ), further suggesting that at high

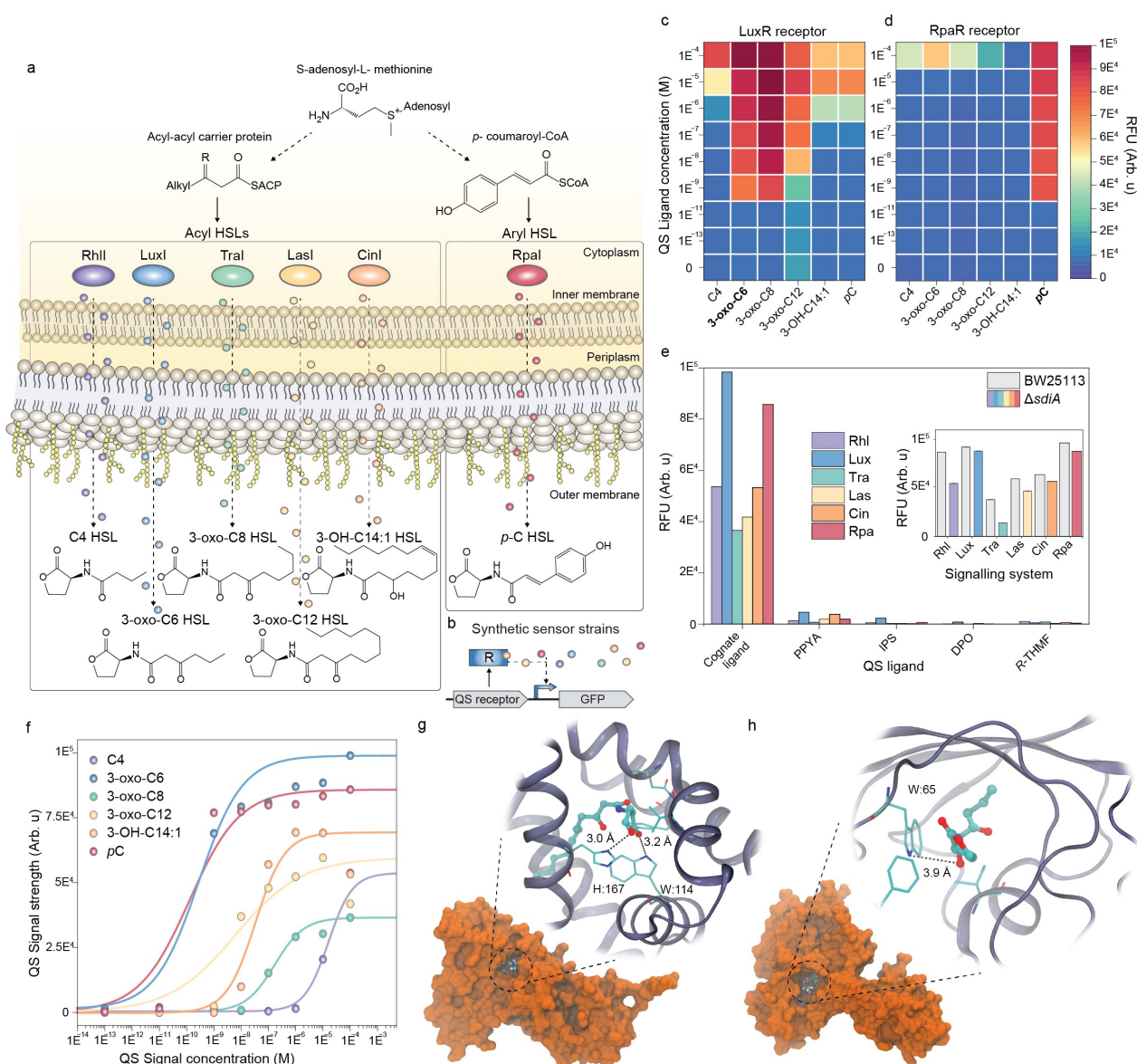


**Figure 3.** Characterization of *N*-acyl and aryl HSL QS signalling systems. **a**) Schematic representation of the *N*-acyl homoserine lactone C4/RhlR, 3-oxo-C6/LuxR, 3-oxo-C8/TraR, 3-oxo-C12/LasR and 3-OH-C14:1/CinR signalling systems from *Pseudomonas aeruginosa*, *Vibrio fischeri*, *Agrobacterium tumefaciens*, *Pseudomonas aeruginosa* and *Rhizobium leguminosarum* respectively, and the aryl homoserine lactone RpaL/RpaR signalling from *Rhodospseudomonas palustris*. **b**) Schematic representation of the synthetic sensor strains used to characterize the QS signalling systems. QS receptors bind to its cognate promoter in the presence of cognate/non-cognate ligands and generate a fluorescent response. **c**) Heatmap characterization of the LuxR signalling system (shown in bold) induced with all HSL ligands, showing high levels of activation, even when activated with non-cognate ligands. The data represent average values of 3 biological replicates. **d**) Heatmap characterization of the Rpa signalling system (shown in bold) induced with all HSL ligands, showing high levels of activation with its cognate ligand and significantly less activation with non-cognate ligands. **e**) The activation of HSL signalling systems with non-HSL ligands shows a large reduction in activation of the HSL systems, indicating that structural diversity in QS ligands is a good indicator for orthogonality. Zoom-in shows a comparison of the maximum induction of the HSL signalling systems with their cognate ligand ( $10^{-4}$  M) in the presence (BW25113) and absence (BW25113  $\Delta$ sdiA) of SdiA, a LuxR homologue orphan, which is found in *E. coli*. **f**) Sensitivity and overall strength of activation of the HSL signalling systems upon addition of external cognate ligand. **g**) Snapshot from 0.5  $\mu$ s long all-atom MD simulations of the LuxR receptor protein shows the strong binding of non-cognate QS ligand 3-oxo-C12 HSL, as seen in (c), within the binding pocket of the receptor protein. **h**) Snapshot from 0.5  $\mu$ s long all-atom MD simulations of the RpaR receptor protein shows the binding of non-cognate QS ligand 3-oxo-C6 HSL, as seen in (d), within the binding pocket of the receptor protein. Water molecules and ions were omitted for clarity in (g) and (h).

concentrations, PauR is toxic to *E. coli*. The addition of 100 nM of *L*-rhamnose enabled the detection of IPS ( $10^{-4}$  M), although the activation was considerably slower and weaker when compared to HSL system activation

(Figure 4c, left/bottom panel). The extra protein induction step and the overall reduced receptor levels likely contribute to the slower and weaker activation. For PluR, the optimal range of activation was achieved in the highest tested *L*-

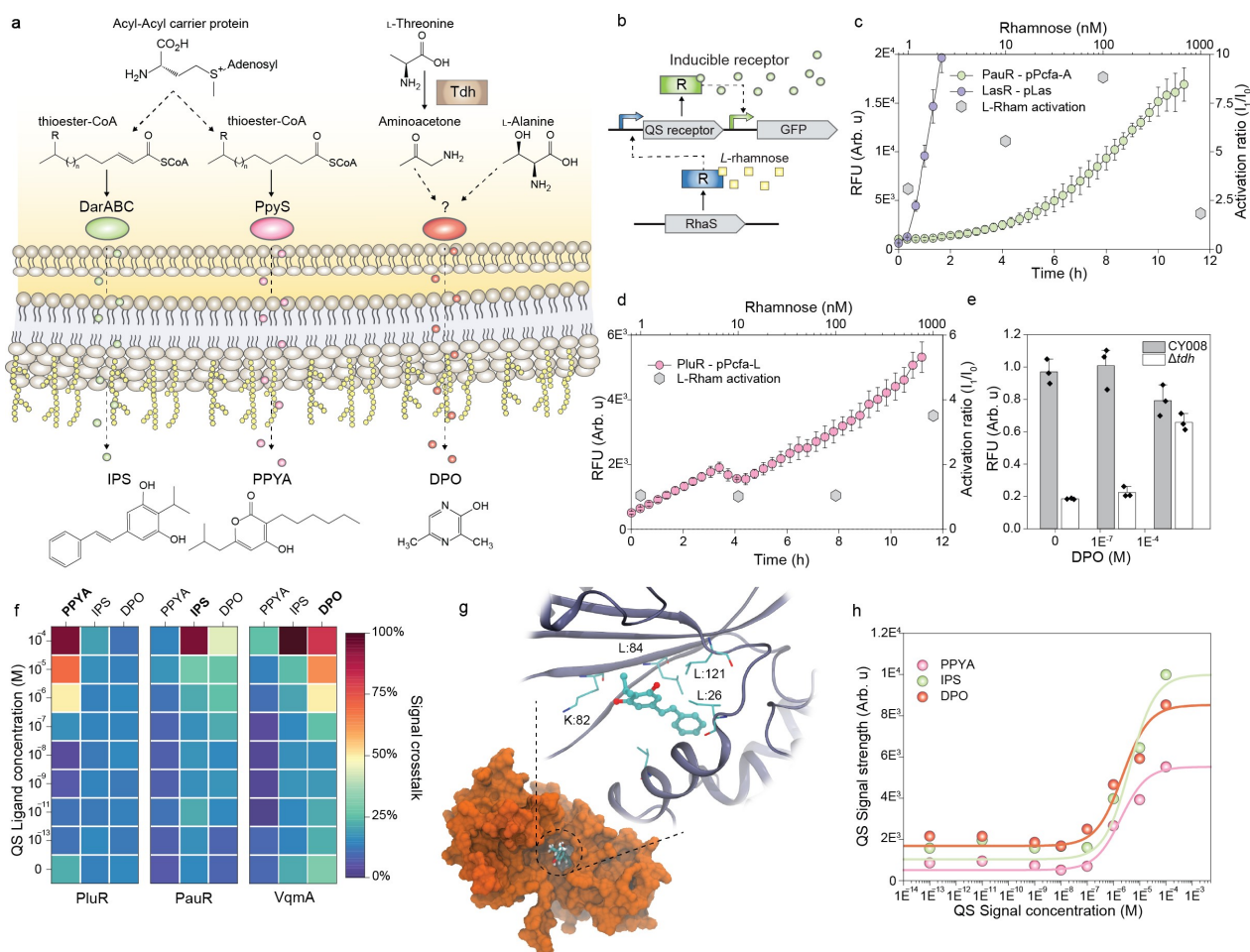


**Figure 4.** Characterization of "Others" categorized QS signalling systems. a) Schematic representation of the IPS/PauR, PPYA/PluR and DPO/VqmA QS signalling systems from *Photobacterium symbiotica*, *Photobacterium luminescens*, and *Vibrio cholerae* respectively. b) Schematic representation of the approach taken to avoid point mutations and create functional signalling systems for DarABC/PauR and PPYA/PluR. An inducible rhamnose promoter was used to regulate the receptor protein expression. c) Activation of the PpcfA-A/PauR reporter system upon the addition of IPS ( $10^{-4}$  M). Because binding of the IPS ligand is dependent on the production of PauR by the rhamnose inducible promoter, the reporter response is considerably slower compared to HSL-based sensors, as illustrated by the comparison with the Las signalling system. The right and top Y and X axis display the activation ratio, characterized as the ratio between induced ( $10^{-4}$  M) and uninduced responses, in different concentrations of L-rhamnose. The data represent average values of biological replicates  $\pm$  s.d. ( $n = 3$  per group). d) Activation of the PpcfA-L/PluR reporter system upon the addition of PPYA ( $10^{-4}$  M) and the activation ratio as seen in different concentrations of L-rhamnose. The data represent average values of biological replicates  $\pm$  s.d. ( $n = 3$  per group). e) Comparison of activity of the DPO/VqmA reporter system in response to varying concentrations of DPO in CY008 and a knockout of the precursor synthase gene  $\Delta tdh$ . The data represent average values of biological replicates  $\pm$  s.d. ( $n = 3$  per group). f) Heatmap activation comparison of the "Other" categorized QS signalling systems. "Other" QS systems were induced with cognate ligand (shown in bold) and other non-cognate ligands from the same class. The data represent average values of 3 biological replicates. g) Snapshot from 0.5  $\mu$ s long all-atom MD simulations of the VqmA receptor protein shows the binding of non-cognate QS ligand IPS, as seen in (f), within the binding pocket of the receptor protein. Water molecules and ions were omitted for clarity. h) Sensitivity and overall strength of activation of the "Others" categorized signalling systems upon addition of external cognate ligand.

rhamnose concentration ( $1 \mu$ M) (Figure 4d). Although no negative effect on growth or activation was observed at this concentration, the range of activation was still lower than observed with PauR. As seen with IPS/PauR, the speed and overall intensity of the PPYA/PluR signalling system was lower compared to HSL-based signalling systems.

Next, we explored another structurally diverse and recently identified QS signalling system, categorized as "Others"; the DPO/VqmA signalling system that controls biofilm formation in *Vibrio cholerae*<sup>21</sup>. The Lux-type receptor VqmA senses DPO, which enables binding to the

promoter *PvqmR*, activating *vqmR*. DPO is produced from threonine catabolism, in a multi-step enzymatic reaction pathway beginning with oxidation of threonine through threonine dehydrogenase (Tdh). Additionally, residual amounts of L-alanine are incorporated into DPO through a minor branch of the synthesis pathway.<sup>[26]</sup> Since DPO production requires Tdh, which is also present in *E. coli*, we constructed the knockout strain  $\Delta tdh$  CY008 to validate the QS system activation. Increasing levels of DPO activated the signalling system in  $\Delta tdh$  (Figure 4e). Unlike the HSL signalling systems (Figure 4b,c), the "Others" categorized



QS systems show minimal activation when challenged with non-cognate ligands (Figure 4f, Figure S3, Supplementary video 3). The only exception is the DPO/VqmA signalling system, where the receptor VqmA is activated by the non-cognate ligand IPS. The activation is even stronger than activation with its cognate ligand. However, where its cognate ligand exhibits a concentration-dependent activation curve, the activation observed with IPS occurs in the highest concentration only ( $1\text{E}^{-4}\text{ M}$ ). We further verified this observation via MD simulations (Supplementary video 4). Figure 4g shows the IPS ligand in the VqmA receptor pocket. However, it should be noted that in contrast to the HSL ligands, here the binding is between aromatic carbons in IPS and aliphatic carbons from three leucines in the VqmA receptor. It is worth to mention that such hydrophobic interactions are the most common in protein-ligand systems.<sup>[27]</sup> A comparison of overall strength and sensitivity shows that sensitivity of the “Others” QS systems is lower than those observed in HSL signalling systems (Figure 4h). Furthermore, the sensitivity of the engineered IPS/PauR and PPYA/PluR QS systems ( $\text{EC}_{50}$  of  $1.93\text{E}^{-6}$  and  $6.68\text{E}^{-6}\text{ M}$  respectively) varies from the activation sensitivity in a natural context.<sup>[9b,24]</sup> Increasing evidence supports that, particularly for HSLs with long branched tails, other transport mechanisms such as fatty acid transporters help facilitate the uptake across bacterial membranes, which could partially explain the differences in dynamic activation ranges.<sup>[28]</sup> Also, the solubility could become limiting at these higher concentrations. Still, as can be seen in Figure 4f, both the PPYA and IPS ligands (which precipitate in high  $1\text{E}^{-3}\text{ M}$  concentrations and above) generate a stronger response at  $1\text{E}^{-4}\text{ M}$  compared to  $1\text{E}^{-5}\text{ M}$  concentrations in the reporter system.

Even though the exact mechanism by which the sensitivity is affected remains unclear to us, similar changes in activation ranges/sensitivity have previously been observed in other adaptations of QS signalling reporter systems depending on the expression organism, expression strain and integration (plasmid or genome).<sup>[22,29]</sup>

The final signalling system we explored is the AI-2 (*R*-THMF)/LsrR signalling system. This system was investigated for several reasons; i) The ligand *R*-THMF exhibits a high similarity with HSLs in the Tanimoto similarity comparison; ii) *R*-THMF is hydrophilic and believed to be membrane impermeable requiring a transporter to pass the cellular membrane; iii) AI-2 signalling is utilized by multiple prokaryotes, both Gram-negative and Gram-positive, as a proposed mechanism of interspecies communication;<sup>[30]</sup> iv) *R*-THMF requires intracellular phosphorylation before it can bind and inhibit its receptor target LsrR; and v) the inhibition of LsrR activates the *Plsr* promoter.<sup>[31]</sup> So, although the predicted structural similarity with HSL ligands is high, the completely different properties and functioning compared to the other QS signalling systems explored in this study make this an interesting candidate for identifying potentially orthogonal systems. *S*-adenosylmethionine (SAM) is converted after several metabolic steps into a homocysteine and 4,5-dihydroxy-2,3-pentanedione (DPD) by the synthase gene *LuxS* (Figure 5a). DPD can convert

spontaneously to different forms depending on the environment, including the active form of AI-2.<sup>[3b,32]</sup>

As with Tdh, *E. coli* produces the synthase *luxS*, so we constructed  $\Delta luxS$  CY008 to validate the QS system activation. We observed very weak activation in response to its cognate ligand. We explored several constructs to strengthen the activation of QS system, where *Plsr* either induced T7 RNA polymerase (pCT5), or both T7 RNA polymerase and LsrR (pCT6) (Figure 5b). As expected, the strongest response was observed in CY008, which contains *LuxS*. However, in both configurations, pCT5 and pCT6, activation levels remained low after the addition of smaller concentrations of external AI-2. This indicates that natural production of AI-2 is low and not sufficient to saturate the binding of the receptor. The largest fold-activation change in response to external AI-2 was observed in the pCT6  $\Delta luxS$  combination, although the overall strength of the QS system remained weak. Next, we used the pCT6  $\Delta luxS$  combination to characterize the effects of non-cognate ligands on the binding (Figure 5c). The Lsr QS system was not activated by any of the non-cognate ligands (Figure 5d). The large differences in the architecture of the AI-2/LsrR signalling systems compared to the other QS signalling systems likely contribute to its low activation by non-cognate ligands. As an example, we ran  $0.5\text{ }\mu\text{s}$  MD simulations of LsrR repressor and 3-OH-C14:1 ligand (Figure 5e). Despite the long simulation time, no specific binding in the LsrR pocket was observed (supplementary video 5). Rather, the ligand is loosely attached to different regions on the protein surface via aliphatic carbons, while its HSL group is exposed to the electrolyte, which can be expected considering the amphiphilic structure of the ligand.

Next, we characterized the compatibility of all experimentally established intercellular signalling systems. When multiple intercellular signals are integrated, interference can occur on different levels. A receptor protein can interact with non-cognate ligands and bind its cognate receptor, which is referred to as signal crosstalk. Particularly LuxR and the LuxR homologue SdiA have been previously reported to bind non-cognate ligands.<sup>[21b,33]</sup> Also, receptor protein-cognate ligand complexes can bind non-cognate promoters, which is referred to as promoter crosstalk. To characterize signal crosstalk, we tried to activate each promoter/receptor pair with all cognate and non-cognate ligands ( $10\times 10$ ) at the highest concentration of  $1\text{E}^{-4}\text{ M}$  (Figure 6a,b). Studying the crosstalk at the highest possible activation concentrations ensures that identified orthogonal QS signalling systems are fully orthogonal across the whole concentration range, since at lower concentrations less crosstalk is encountered. As previously reported, crosstalk is prevalent in the HSL signalling systems, with particularly the *Plux*/LuxR promoter/receptor pair showing activation in response to a wide variety of non-cognate QS ligands. Apart from CinR, all HSL-based receptor proteins were activated by non-cognate HSL ligands. Interestingly, the non-HSL ligands did not activate any of the HSL signalling systems. Furthermore, the non-HSL signalling systems showed low levels of crosstalk among themselves. A notable exception was observed for receptor protein VqmA, where activation



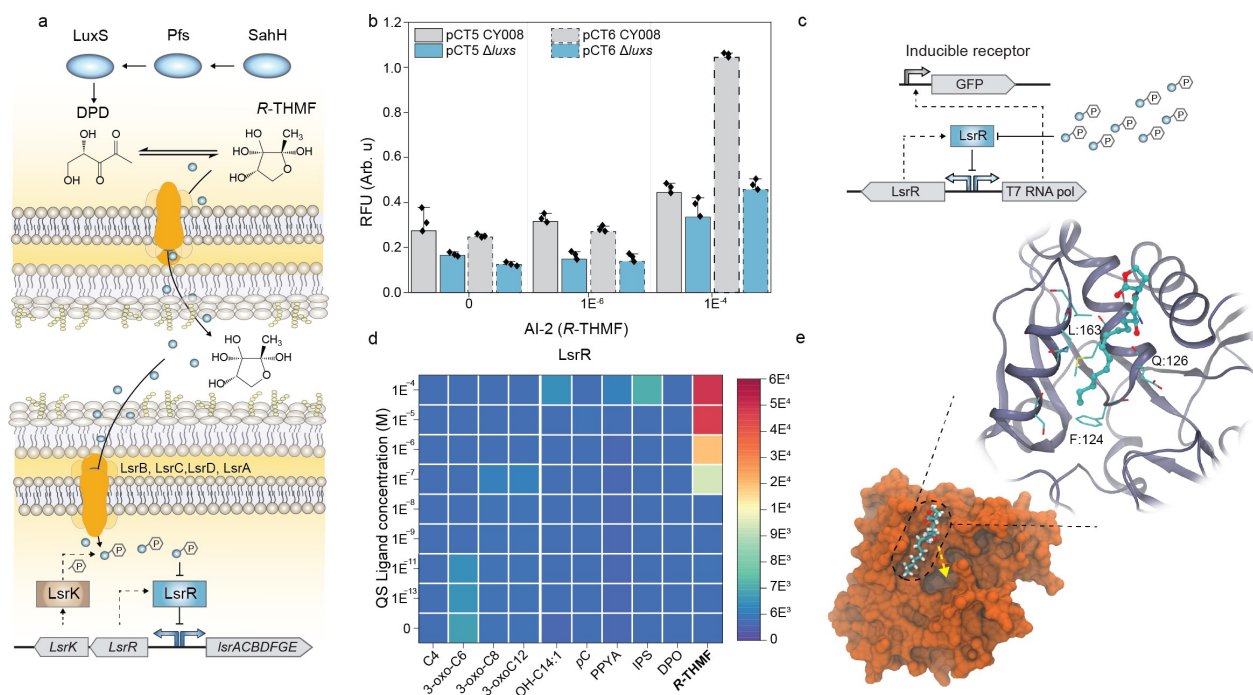


**Figure 5.** Characterization of AI-2/LsrR QS signalling system. a) Schematic representation of the AI-2/LsrR QS signalling system, which is utilized in multiple prokaryotes, both Gram-positive and Gram-negative. b) Comparison of activity of the *Plsr/LsrR* reporter system in response to varying concentrations of AI-2 (R-THMF) in CY008 and a strain containing a knockout ( $\Delta luxS$ ) of the synthase gene *LuxS*. Two variations were tested; in pCT5, the *Plsr* promoter induces T7 polymerase, which activates a response; in pCT6 the *Plsr* promoter induces T7 polymerase, as well as the production of more LsrR. The data represent average values of biological replicates  $\pm$  s.d. ( $n = 3$  per group). c) Schematic representation of the experimental method used to characterize the AI-2 QS signalling system. The QS repressor LsrR binds phosphorylated AI-2, promoting the production of more LsrR as well as T7 RNA polymerase, which activates the response. d) Heatmap of the activation of the AI-2/LsrR signalling system (shown in bold) induced with all QS ligands, shows moderate levels of activation with its cognate ligand and very low activation with all other non-cognate ligands. The data represent average values of 3 biological replicates. e) Snapshot from 0.5  $\mu$ s long all-atom MD simulations of the LsrR repressor shows that non-cognate QS ligands, such as 3-OH-C14:1, do not bind within the binding pocket of the receptor protein. The yellow line highlights the LsrR binding pocket. Water molecules and ions were omitted for clarity.

with non-cognate ligand IPS was considerably more potent than with cognate ligand DPO. A comparison of the signal crosstalk heatmap with the ligand ECFP score overlap heatmap shows a similar signature, with lots of overlap between HSL systems, limited-to-no overlap between HSL and non-HSL systems, and limited overlap between non-HSL signalling systems (Figure 6a, Figure S4). This suggests that diversity in ligand chemical structures (calculated by ECFPs and clustered using UMAP dimensionality reduction) can serve as a powerful tool to predict non-cognate interactions. The signal crosstalk analysis generated a set of six signal-orthogonal QS intercellular signalling systems, including three out of four non-HSL systems (Figure 6a, zoom-in dashed lines).

To characterize promoter crosstalk, we tried to activate each promoter with all cognate and non-cognate receptor-ligand complexes (10x10 combinations) (Figure 6c,d). Promoter crosstalk activation was far less prevalent when compared to signalling crosstalk activation among HSL signalling systems. However, the LuxR-3-oxo-C6 complex was able to strongly bind and activate a variety of promoters, notably *Prhl*, *Prpa*, *PpcfA-L* and *PpcfA-A*. Particularly the binding to promoter *PpcfA-A* is of interest, as the binding is considerably stronger than the binding by

its cognate receptor-ligand complex. The promoter crosstalk analysis generated a set of seven promoter-orthogonal QS intercellular signalling systems, including all six signal orthogonal systems, C4//RhIR, 3-oxo-C8//TraR, 3OH-C14:1/CinR, PPYA//PluR, DPO/VqmA and AI-2/LsrR, as well as 3-oxo-C12/LasR (Figure 6c, zoom-in dashed lines). Further examination of crosstalk at more naturally relevant concentrations of QS ligand,  $10^{-8}$  and  $10^{-11}$  M, shows less crosstalk, as expected (Figure S5). However, these concentrations, particularly in the case of  $10^{-11}$  M, drop below the activation range of some QS signalling systems. For IPS/PauR, DPO/VqmA and AI-2/LsrR,  $10^{-8}$  M of ligand already drops below the activation range of these QS signalling systems. Lastly, we compared a range of characteristics of each experimentally validated QS signalling system that affects their overall functionality/usability. We compared ligand structural similarity (calculated by ECFP distances) (Figure 6e), the speed and sensitivity of activation (both defined at  $EC_{50}$ ) (Figure 6f,g, respectively), the overall activation strength (Figure 6h), the level of non-cognate ligand binding (Figure 6i), the level of non-cognate promoter activation (Figure 6j) and the presence of conserved amino acids within the AHL binding domain (Figure 6k), compared to all other experimentally

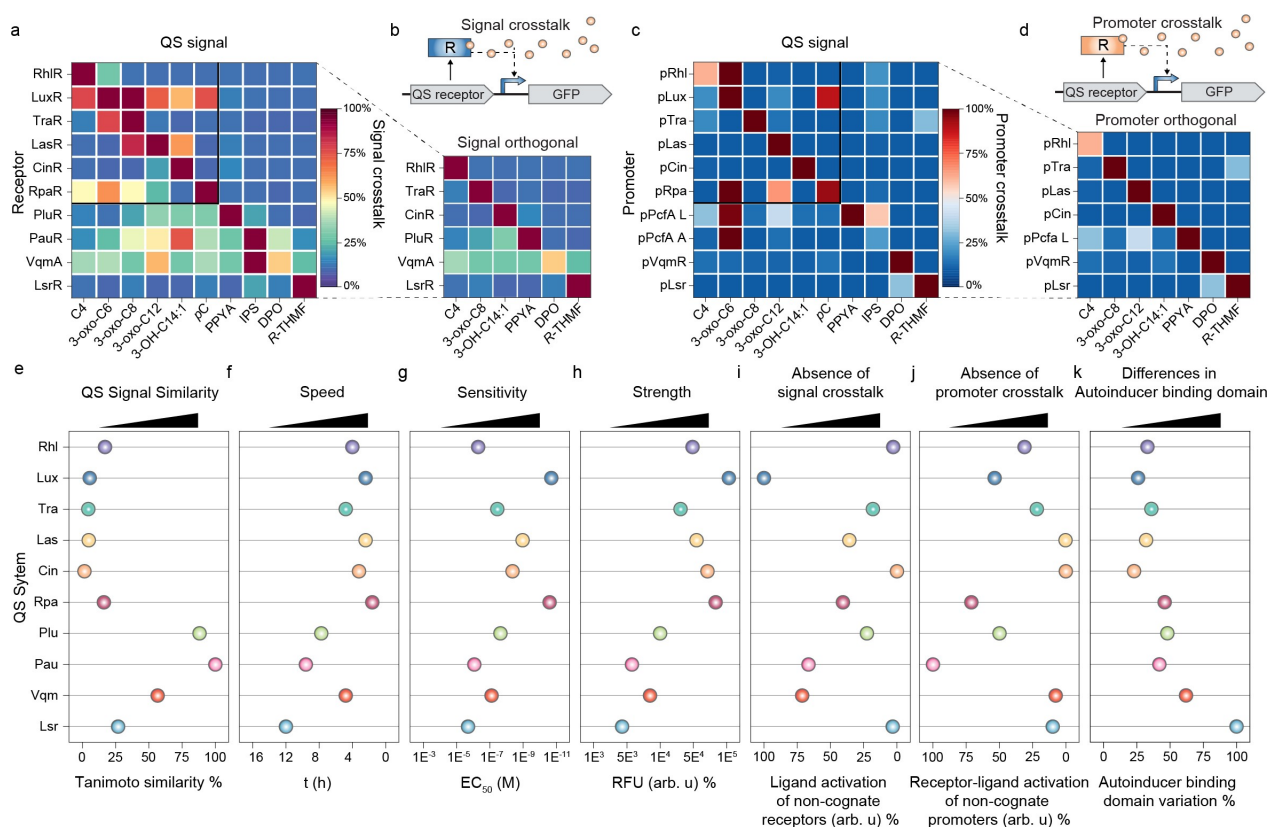


**Figure 6.** Comparison of properties of QS signalling systems and characterization of crosstalk. a) Heatmap characterization of the overlap observed when QS signalling systems are induced with non-cognate ligands, referred to as signal crosstalk. The heatmap was constructed using the highest ( $10^{-4}$  M) concentration of ligands. Solid black lines mark the HSL signalling systems. Dashed black lines (zoom-in) show the selection of QS signalling systems which are signal orthogonal. Signal orthogonal systems are defined as non-cognate signal recognition and activation remaining under 33 % of maximum, when compared with cognate ligand. The data represent average values of 3 biological replicates. b) Schematic representation of the experimental method used to characterize signal crosstalk between the QS signalling systems. A QS receptor with cognate QS promoter is challenged with non-cognate ligands. The binding of QS receptors to its cognate promoter in the presence of non-cognate ligands is referred to as signal crosstalk. c) Heatmap characterization of the overlap observed when a signalling ligand together with its cognate receptor binds to a non-cognate promoter, referred to as promoter crosstalk. Black lines mark the HSL signalling systems. Dashed black lines (zoom-in) show the selection of QS signalling systems which are promoter orthogonal. Promoter orthogonal systems are defined as promoter binding and activation in response to non-cognate ligand/receptor protein complexes remaining under 33 % of maximum, when compared with its cognate ligand/receptor complex. The data represent average values of 3 biological replicates. d) Schematic representation of the experimental method used to characterize promoter crosstalk. A QS receptor is challenged with its cognate ligand in the presence of a non-cognate promoter. The binding of QS receptors to non-cognate promoters is referred to as promoter crosstalk. e) Scaled Tanimoto similarity between all experimentally studied QS signalling systems. f) Activation speed of QS signalling systems after challenging with cognate QS ligand. g) Sensitivity of QS systems, defined as concentration of ligand (M) required to reach 50 % of maximum activation. h) Strength of the QS systems, scaled in arbitrary units. i) Scaled signal crosstalk of each QS receptor and cognate promoter with all non-cognate ligands (0–100 %). j) Scaled promoter crosstalk of each QS promoter with all other non-cognate receptor-ligands (0–100 %). The data shown in (f,g,h,i,j) represent average values of 3 biological replicates. k) Scaled presence of conserved amino acids (75–100 %) in the AHL-domain (autoind\_bind, PFAM03472) of all experimentally studied QS receptor proteins. For visual clarity, in all graphs (e–k) the desirable property of the QS signalling system is plotted towards the right side, resulting in the occasional inverse scale in (f,g,h,i,j) on the x-axis.

verified signalling systems. This detailed characterization helps with the selection of QS intercellular signalling systems in biotechnological community-wide engineering approaches.

## Conclusion

QS signalling systems are ubiquitous in prokaryotes, and novel QS ligands are continually being identified.<sup>[26,34]</sup> Furthermore, increasing evidence alludes to interspecies and

even interkingdom signalling systems, expanding the range, scope, and complexity of intercellular signal recognition.<sup>[30]</sup> However, a key challenge that remains is the understanding of non-cognate interactions between QS signalling systems, both for understanding the interactions and interdependencies in natural communities, as well as for the utilization of these QS signalling systems to engineer community-wide behaviour. The high degrees of overlap in ligand chemical structures,<sup>[25]</sup> the possibility of multiple (and interconnected) signalling systems being utilized by a single bacterium simultaneously,<sup>[35]</sup> the presence of conserved binding do-

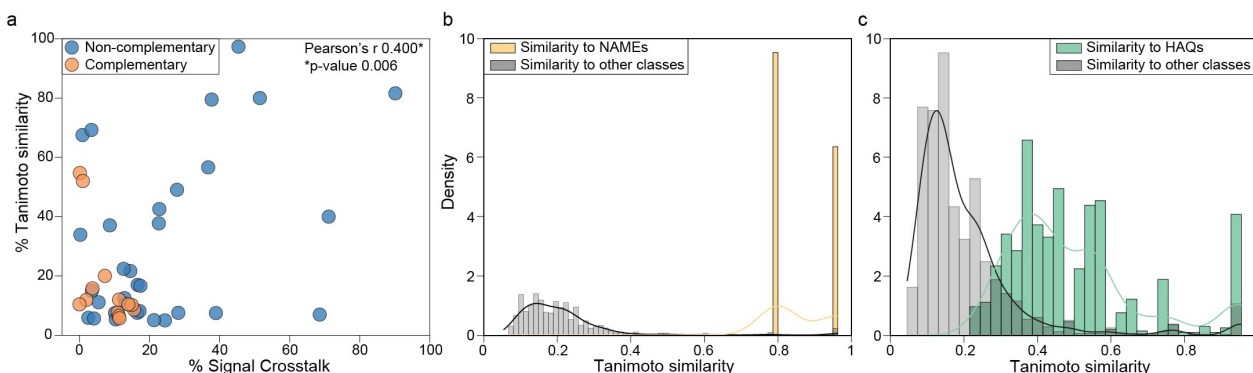


**Figure 7.** Exploration of chemical space using ECFP and UMAP approximations. a) Pearson correlation between calculated Tanimoto similarities and measured signal crosstalk values. Significant correlation was observed between ligand diversity and experimental crosstalk values. Highlighted in orange are the experimentally verified complementary systems as seen in the zoom-ins in Figure 6a,c. b) Similarity comparison between NAMEs and all other QS ligands shows a high degree of overlap among individual NAME ligands, indicating a high degree chemical similarity of ligands within its class. NAME ligands show a very low similarity to QS ligands in other classes. c) Similarity comparison between HAQs and all other QS ligands shows a wide range of overlap among individual HAQ ligands, indicating more diversity in chemical structures of ligands within its class. HAQ ligands show a low similarity to QS ligands in other classes.

mains that are shared in receptor proteins,<sup>[36]</sup> and the presence of orphan/solo receptor proteins (which lack a cognate ligand, but which often bind non-cognate ligands)<sup>[37]</sup> all add to this complexity.

Here, we hypothesized that structural diversity in QS ligand chemical structure serves as a good starting point for the prediction of overlap and non-cognate receptor-ligand binding in QS intercellular signalling systems. We explored the use of dimensionality reduction by UMAP on a bulk collection of QS ligands using ECFP fingerprinting as a tool to help identify unexplored areas in the ligand chemical space. UMAP dimensionality reduction excels at capturing local as well as global structural similarities and differences within groups/subgroups and between distinct groups of signalling molecules.<sup>[14b]</sup> We first investigate, and experimentally verify, a set of highly similar HSL QS signalling ligands and find that non-cognate receptor-ligand binding is frequently observed (Figure 3c,d,g,h, Figure 5a), in line with previous observations.<sup>[22]</sup> Also, via all-atom MD simulations, we verified and characterized experimentally observed non-cognate binding in the representative signalling systems. As we moved to more structurally diverse ligands, we observed that these ligands cannot activate any of the HSL QS signalling systems (Figure 3e). Since the ligand structural diversity is far larger within the category “Others”, we observed limited activation through non-cognate interactions. Similarly, the AI-2/R-THMF signalling system, which differs from other systems in functionality, shows no non-cognate binding of either the ligand (AI-2) or the receptor (LsrR).

Finally, we examined how the simple mapping of chemical diversity in ligands can predict and understand receptor-ligand binding interactions by comparing the calculated Tanimoto similarity values with the experimentally characterized signal crosstalk between the QS signalling systems (Figure 7a). A comparison demonstrates a statistically significant correlation between the datasets ( $p\text{-value} = 0.006$ ). Furthermore, a comparison between non-cognate

receptor-ligand binding (Figure 6a) and ECFP & UMAP ligand diversity scores (Figure S4) shows a comparable overall organization of heatmap patterns. We also identified potentially interesting unexplored areas of ligand chemical space, particularly in the NAMEs and HAQs (Figure 7b,c) and to a lesser extent in the DSFs and DKPs (Figure S6a,b). NAMEs, HAQs and DSFs show no overlap with other classes of QS ligands and particularly NAMEs and DSFs show a high degree of ligand similarity within its class. Conversely, the HAQs show a larger degree of variation of ligand similarity within its class. The low similarity of these QS classes with other classes makes them interesting starting points for future attempts to characterize additional synthetic orthogonal QS systems.

Altogether, these results support our hypothesis that structural diversity in QS ligand chemical structure serves as a good starting point for the prediction of overlap and non-cognate receptor-ligand binding in QS intercellular signalling systems. This further highlights the potential of utilizing computational tools to explore biological phenomena like receptor-ligand interactions without extensive prior characterization and provides a clear strategy towards the future identification of additional orthogonal intercellular QS signalling systems.

### Author Contributions

Conceptualization, C.J., P.S., E.O. and M.B.L.; Methodology, C.J., P.S., J.V.S. and P.B.; Analysis, C.J., P.S., J.V.S., E.O. and P.B.; Writing, C.J. and P.S.; Review and editing, E.O. and M.B.L.

### Acknowledgements

The authors would like to acknowledge funding from the Academy of Finland through its Centre of Excellence



Programme Life-Inspired Hybrid Materials (LIBER 2022–2029, grant 346105: C.J., E.O., M.B.L.) and Academy Projects (grant 272578: C.J., E.O., M.B.L.). P.B. would like to thank the European Union Erasmus+ Programme (project no: 2019-1-PL01-KA103-061592) for providing financial support for the mobility and training in Aalto University. We gratefully acknowledge Poland's high-performance computing infrastructure PLGrid (HPC Centers: ACK Cyfronet AGH) for providing computer facilities and support within computational grant no. PLG/2023/016229. We would like to thank Professor Helge B. Bode and Peter Grün, for providing the QS ligands DAR IPS, PPYA and PPYB. We would like to thank Prof. Ralf Heermann, for the sharing of plasmids containing PluR, PauR and promoter sequences. Furthermore, we would like to thank the Coil Genetic Stock Center (CGSC) for the Keio *E. coli* knockout strains. Finally, we would like to thank Dr. Georg Schmidt, Meryem Ecem Kaya and Saleh Khan for the input and discussions.

### Conflict of Interest

The authors declare no conflict of interest.

### Data Availability Statement

The data that support the findings of this study is available within the main text and its Supporting Information file and Supporting Information Table 1.

**Keywords:** Chemical Biology • Molecular Dynamics • Quorum-Sensing • Receptor-Ligand Interactions • Structural Fingerprinting

- [1] B. P. Teague, R. Weiss, *Science* **2015**, *349*, 924–925.
- [2] a) M.-T. Chen, R. Weiss, *Nat. Biotechnol.* **2005**, *23*, 1551–1555; b) A. Camilli, B. L. Bassler, *Science* **2006**, *311*, 1113–1116; c) C. M. Waters, B. L. Bassler, *Annu. Rev. Cell Dev. Biol.* **2005**, *21*, 319–346; d) C. Jonkergouw, N. K. Beyeh, E. Osmekhina, K. Leskinen, S. M. Taimoory, D. Fedorov, E. Anaya-Plaza, M. A. Kostianen, J. F. Trant, R. H. A. Ras, P. Saavalainen, M. B. Linder, *Nat. Commun.* **2023**, *14*, 2141.
- [3] a) Y.-M. Shi, H. B. Bode, *Nat. Chem. Biol.* **2017**, *13*, 453–454; b) R. Daniels, J. Vanderleyden, J. Michiels, *FEMS Microbiol. Rev.* **2004**, *28*, 261–289.
- [4] a) S. Genin, T. P. Denny, *Annu. Rev. Phytopathol.* **2012**, *50*, 67–89; b) A. L. Schaefer, E. P. Greenberg, C. M. Oliver, Y. Oda, J. J. Huang, G. Bittan-Banin, C. M. Peres, S. Schmidt, K. Juhaszova, J. R. Sufrin, C. S. Harwood, *Nature* **2008**, *454*, 595–599.
- [5] a) S. W. Dickey, G. Y. C. Cheung, M. Otto, *Nat. Rev. Drug Discovery* **2017**, *16*, 457–471; b) B. Rada, T. L. Leto, *Trends Microbiol.* **2013**, *21*, 73–81.
- [6] a) P. Bittihn, M. O. Din, L. S. Tsimring, J. Hastly, *Curr. Opin. Microbiol.* **2018**, *45*, 92–99; b) C. Schmidt, *Nature* **2015**, *518*, S12–S14.
- [7] T. R. Zuroff, W. R. Curtis, *Appl. Microbiol. Biotechnol.* **2012**, *93*, 1423–1435.
- [8] a) A. Tamsir, J. J. Tabor, C. A. Voigt, *Nature* **2011**, *469*, 212–215; b) P. Siuti, J. Yazbek, T. K. Lu, *Nat. Biotechnol.* **2013**, *31*, 448–452; c) E. Osmekhina, C. Jonkergouw, G. Schmidt, F. Jahangiri, V. Jokinen, S. Franssila, M. B. Linder, *Commun. Biol.* **2018**, *1*, 97.
- [9] a) K. Papenfort, K. U. Förstner, J.-P. Cong, C. M. Sharma, B. L. Bassler, *Proc. Natl. Acad. Sci. USA* **2015**, *112*, E766–E775; b) S. Brameyer, D. Kresovic, H. B. Bode, R. Heermann, *Proc. Natl. Acad. Sci. USA* **2015**, *112*, 572–577; c) K. Papenfort, J. E. Silpe, K. R. Schramma, J.-P. Cong, M. R. Seyedasayam-dost, B. L. Bassler, *Nat. Chem. Biol.* **2017**, *13*, 551–557.
- [10] A. M. Tsou, T. Cai, Z. Liu, J. Zhu, R. V. Kulkarni, *Nucleic Acids Res.* **2009**, *37*, 2747–2756.
- [11] J. P. Ramsay, T. R. Bastholm, C. J. Verdonk, D. D. Tambalo, J. T. Sullivan, L. K. Harold, B. A. Panganiban, E. Colombi, B. J. Perry, W. Jowsey, C. Morris, M. F. Hynes, C. S. Bond, A. D. S. Cameron, C. K. Yost, C. W. Ronson, *Nucleic Acids Res.* **2022**, *50*, 975–988.
- [12] A. Rajput, K. Kaur, M. Kumar, *Nucleic Acids Res.* **2016**, *44*, D634–D639.
- [13] D. Rogers, M. Hahn, *J. Chem. Inf. Model.* **2010**, *50*, 742–754.
- [14] a) M. W. Dorrity, L. M. Saunders, C. Queitsch, S. Fields, C. Trapnell, *Nat. Commun.* **2020**, *11*, 1537; b) M. Karimzadeh, C. Ernst, A. Kundaje, M. M. Hoffman, *Nucleic Acids Res.* **2018**, *46*, e120–e120.
- [15] A. Vannini, C. Volpari, C. Gargioli, E. Muraglia, R. Cortese, R. De Francesco, P. Neddermann, S. Di Marco, *EMBO J.* **2002**, *21*, 4393–4401.
- [16] a) T. S. Moon, C. Lou, A. Tamsir, B. C. Stanton, C. A. Voigt, *Nature* **2012**, *491*, 249–253; b) D. Song, J. Meng, J. Cheng, Z. Fan, P. Chen, H. Ruan, Z. Tu, N. Kang, N. Li, Y. Xu, X. Wang, F. Shu, L. Mu, T. Li, W. Ren, X. Lin, J. Zhu, X. Fang, M. W. Amrein, W. Wu, L.-T. Yan, J. Lü, T. Xia, Y. Shi, *Nat. Microbiol.* **2019**, *4*, 97–111.
- [17] B. B. Rutherford ST, *Cold Spring Harbor Perspect. Med.* **2012**, *2*, a012427.
- [18] a) R.-G. Zhang, K. M. Pappas, J. L. Brace, P. C. Miller, T. Oulmassov, J. M. Molyneaux, J. C. Anderson, J. K. Bashkin, S. C. Winans, A. Joachimiak, *Nature* **2002**, *417*, 971–974; b) C. Grandclément, M. Tannières, S. Moréra, Y. Dessaux, D. Faure, *FEMS Microbiol. Rev.* **2016**, *40*, 86–116.
- [19] a) E. González Juan, M. Marketon Melanie, *Microbiol. Mol. Biol. Rev.* **2003**, *67*, 574–592; b) J. K. Lithgow, A. Wilkinson, A. Hardman, B. Rodelas, F. Wisniewski-Dyé, P. Williams, J. A. Downie, *Mol. Microbiol.* **2000**, *37*, 81–97; c) B. Rodelas, K. Lithgow James, F. Wisniewski-Dye, A. Hardman, A. Wilkinson, A. Economou, P. Williams, J. A. Downie, *J. Bacteriol.* **1999**, *181*, 3816–3823.
- [20] L. Mellbye Brett, J. Bottomley Peter, A. Sayavedra-Soto Luis, *Appl. Environ. Microbiol.* **2015**, *81*, 5917–5926.
- [21] a) M. J. Bottomley, E. Muraglia, R. Bazzo, A. Carfi, *J. Biol. Chem.* **2007**, *282*, 13592–13600; b) A. Lindsay, M. M. Ahmer Brian, *J. Bacteriol.* **2005**, *187*, 5054–5058.
- [22] N. Kylilis, Z. A. Tuza, G.-B. Stan, K. M. Polizzi, *Nat. Commun.* **2018**, *9*, 2677.
- [23] A. O. Brachmann, S. Brameyer, D. Kresovic, I. Hitkova, Y. Kopp, C. Manske, K. Schubert, H. B. Bode, R. Heermann, *Nat. Chem. Biol.* **2013**, *9*, 573–578.
- [24] S. Brameyer, H. B. Bode, R. Heermann, *Trends Microbiol.* **2015**, *23*, 521–523.
- [25] H. Wu, M. Li, H. Guo, H. Zhou, B. Li, Q. Xu, C. Xu, F. Yu, J. He, *J. Biol. Chem.* **2019**, *294*, 2580–5171.
- [26] R. Ferreira de Freitas, M. Schapira, *MedChemComm* **2017**, *8*, 1970–1981.
- [27] E. Krol, A. Becker, *Proc. Natl. Acad. Sci. USA* **2014**, *111*, 10702–10707.
- [28] a) A. J. Meyer, T. H. Segall-Shapiro, E. Glassey, J. Zhang, C. A. Voigt, *Nat. Chem. Biol.* **2019**, *15*, 196–204; b) C. A. Vaiana, H. Kim, J. Cottet, K. Oai, Z. Ge, K. Conforti, A. M.



- King, A. J. Meyer, H. Chen, C. A. Voigt, C. R. Buie, *Mol. Syst. Biol.* **2022**, *18*, e10785.
- [29] J.-H. Lee, T. K. Wood, J. Lee, *Trends Microbiol.* **2015**, *23*, 707–718.
- [30] K. Kamaraju, J. Smith, J. Wang, V. Roy, H. O. Sintim, W. E. Bentley, S. Sukharev, *Biochemistry* **2011**, *50*, 6983–6993.
- [31] T. Xue, L. Zhao, H. Sun, X. Zhou, B. Sun, *Cell Res.* **2009**, *19*, 1258–1268.
- [32] a) G. Chen, L. R. Swem, D. L. Swem, D. L. Stauff, C. T. O'Loughlin, P. D. Jeffrey, B. L. Bassler, F. M. Hughson, *Mol. Cell* **2011**, *42*, 199–209; b) D. J. Schu, R. Ramachandran, J. S. Geissinger, A. M. Stevens, *J. Bacteriol.* **2011**, *193*, 6315–6322.
- [33] V. C. Scoffone, L. R. Chiarelli, V. Makarov, G. Brackman, A. Israyilova, A. Azzalin, F. Forneris, O. Riabova, S. Savina, T. Coenye, G. Riccardi, S. Buroni, *Sci. Rep.* **2016**, *6*, 32487.
- [34] K. Papenfort, B. L. Bassler, *Nat. Rev. Microbiol.* **2016**, *14*, 576–588.
- [35] S. Brameyer, R. Heermann, *PLoS One* **2015**, *10*, e0124093.
- [36] S. Subramoni, D. V. Florez Salcedo, Z. R. Suarez-Moreno, *Front. Cell. Infect. Microbiol.* **2015**, *5*, 00016.
- [37] S. R. Scott, J. Hasty, *ACS Synth. Biol.* **2016**, *5*, 969–977.

Manuscript received: September 26, 2023

Accepted manuscript online: October 25, 2023

Version of record online: November 10, 2023